

## Supplementary Information

# In-vitro quantification of botulinum neurotoxin type A1 using immobilized nerve cell-mimicking nanoreactors in a microfluidics platform

*Oliver G. Weingart,<sup>1,2+</sup> Klaus Eyer,<sup>3,4+\*</sup> Christian Lüchtenborg,<sup>5</sup> Timo Sachsenheimer,<sup>5</sup> Britta Brügger,<sup>5</sup> Marc van Oostrum,<sup>6</sup> Bernd Wollscheid,<sup>6</sup> Petra S. Dittrich,<sup>3</sup> Martin J. Loessner<sup>1</sup>*

**FRET-substrate in NMN.** Comparison of the SNAPtide content in an NMN suspension to a standard curve showed that the suspension contains substrate in a concentration of roughly 2.2  $\mu\text{M}$  (Fig. 2f), which corresponds to an encapsulation efficiency (EE) of 2.75%. The SNAPtide molecules are restricted to the volume of the liposomes that is approximately 3.8% of the volume in the suspension. Accordingly, the SNAPtide concentration within the liposomes is 57.9  $\mu\text{M}$ , i.e. approximately 25 SNAPtide molecules are entrapped in a liposome, which corresponds to SNAPtide concentrations used to measure BoNT/A activity in other studies.

**Liposome stability.** Change in particle size can be an indicator of liposome physical instability, as long-term storage can lead to aggregation or fusion of liposomes thus causing an increase in the hydrodynamic diameter. For newly produced, functionalized liposomes, we determined an average hydrodynamic diameter of 139.1 nm with a polydispersity of 0.07 (Fig. 2g), indicating a monodisperse distribution of liposomal vesicles with a narrow size distribution. Functionalized liposomes were used within 30 days after production. However, even after 30 days of storage at 4°C, the average hydrodynamic diameter increased only slightly, and the low polydispersity value still indicated a stable, monodisperse formulation. Significant change of the size distribution was only observed after prolonged storage.

**Lipid analysis of NMN.** Lipid analysis of NMN produced from a porcine brain total lipid extract (Avanti Polar Lipids, Alabaster, USA) was performed by mass spectrometry and thin layer chromatography. A 1 mM solution in chloroform was diluted to 100  $\mu\text{M}$ . Phosphate determination was done as described<sup>26</sup>, yielding a phospholipid concentration of 51.8  $\mu\text{M}$ . NMN phospholipids, neutral lipids and cholesterol were subjected to an acidic extraction in the presence of internal lipid standards, except for plasmalogen which were extracted under neutral conditions<sup>26</sup>. Mass spectrometric lipid analyses were performed in positive ion mode on an AB SCIEX QTRAP 5500

mass spectrometer using chip-based electrospray infusion and ionization via a Triversa Nanomate (Advion Biosciences, Ithaca, USA) as previously described<sup>26</sup>. Ganglioside extraction and purification for thin layer chromatography and mass spectrometry was performed according to Garcia et al.<sup>27</sup>. For single-step extractions dried down lipids were reconstituted in 1.3 ml chloroform/methanol/water (30/60/8, vol/vol/vol). Following centrifugation for 5 min at 15.000g and RT, the supernatant was transferred to a new tube, while the pellet was subjected to a second extraction. Supernatants were dried under a gentle stream of nitrogen gas. For solid phase extractions, Supelco C8 SPE cartridges (Sigma-Aldrich, St. Louis, USA) were washed with 3 ml methanol and conditioned with 2 ml 60% methanol. Sample was resuspended in 1 ml 60% methanol and applied to the column. The flow through was reapplied and the column was washed with 3 ml 60% methanol. Gangliosides were eluted with 4 ml neat methanol. Eluates were dried under a gentle stream of nitrogen gas. For thin layer chromatography analysis of gangliosides, samples were evaporated and resuspended in methanol and spotted via Linomat Camaq sample spotter (Camag AG, Mutenz, Switzerland) using a Hamilton syringe as described previously<sup>28</sup>. As mobile phase chloroform/methanol/0.25% aqueous potassium chloride (60:35:8, vol/vol/vol) was used. Gangliosides were detected using a sialic acid-sensitive resorcinol reagent<sup>28</sup>. A brain ganglioside standard (mixed gangliosides, purified bovine (#1065; Matreya, Pleasant Gap, USA) was used as reference. For mass spectrometric analysis of gangliosides, 50 pmol each of GM3 and GM1 (18:0-D3 species; Matreya, Pleasant Gap, USA) were used as internal lipid standards. Gangliosides were subjected to UHPLC-MS analysis, using a CHS C18 column (2.1x100mm, 1.7 µm particles, Waters, Milford, USA) coupled to a QExactive high resolutions Orbitrap mass spectrometer (ThermoFisher Scientific, Waltham, USA) equipped with an HESI source. Prior to measurement the evaporated samples were resuspended in 50 µl LC buffer 1 containing 60% of mobile phase A (acetonitrile:water; 60:40 (vol:vol) in 10 mM ammonium formate and 0.1% formic acid) and 40% mobile phase B (isopropanol:acetonitrile, 90:10 (vol:vol) in 10 mM ammonium formate and 0.1% formic acid). 30 µl of each sample was subjected to UPLC separation (Dionex, Sunnyvale, USA), using a step gradient of 60–57% A (0.0–2.0 min), 57–50% A (2.0–2.1 min), 50-46% A (2.1-12.0 min), 46-30% A (12.0-12.1 min), 30-1% A (12.1-18.0 min), 1-60% A (18.0-18.1) and 60% A (18.1-20.0 min). The column temperature was set to 55°C and the flow rate to 0.1 ml/min. Full MS scans were acquired for 30 min in negative ion mode (600-1800 m/z) were with automatic gain control target of 1x10<sup>6</sup> ions, maximal injection time of 200 ms and resolution set to 140,000. All ion fragmentation in negative ion mode was performed at a resolution of 70,000, scanning a mass range of 120-600 m/z with normalized collision energy set to 30 eV. Data evaluation was performed using MassMap (MassMap, Wolfratshausen, Germany). Raw files were converted to Mzxml-files with ms-

convert. MassMap was used to convert these files to nmp-files. Full-scans and fragmentation-scans were separated with MassMap. A type2 baseline correction was done. Full MS scans were evaluated with lis-par file for GM1, GM3, GD1, including IS with chain lengths of 34-44, double bonds 1-2, 1- to 3-hydroxylations. GM1 and GD1 intensities was quantified with intensity of IS GM1-D3. Calculations were performed in excel. Species distribution was calculated and average for 518, 1036 and 1554 pmol pi of NMN extract was calculated.

**Protein analysis of NMN.** For protein analysis, NMN were resuspended in lysis buffer consisting of 1 M guanidine, 10% Acetonitrile, 50 mM Ammonium bicarbonate (Sigma-Aldrich, St. Louis, USA) and 0.5% RapiGest, sonicated three times for one minute and diluted with 6 volumes of ice-cold acetone and incubated at -20 C overnight. The mixture was then centrifuged for 10 minutes at 15'000 g and the resulting pellet reconstituted in lysis buffer, reduced for 30 minutes at 37°C with 5 mM TCEP (Sigma-Aldrich, St. Louis, USA), alkylated for 30 minutes at ambient temperature using 10 mM iodacetamine (Sigma-Aldrich, St. Louis, USA) and subsequently digested with LysC (Wako, Neuss, Germany) and trypsin (Promega, Dübendorf, Switzerland). After digestion, the peptide mixture was acidified by adding 0.1% formic acid, incubated at 37°C for 30 minutes and centrifuged at 20'000 g for 10 minutes. The supernatant was desalted on an Oasis MCX extraction cartridge (Waters, Milford, USA) according to the manufacturer's instructions and dried in a SpeedVac concentrator (Thermo Scientific, Rockford, USA). For MS analysis, peptides were reconstituted in 2% acetonitrile, 0.1% formic acid and separated by reversed-phase chromatography on a high pressure liquid chromatography (HPLC) column (75- $\mu$ m inner diameter; New Objective, Woburn, USA) packed in-house with a 15-cm stationary phase (Magic C18AQ, 200 Å, 1.9; Michrom Bioresources, Auburn, USA) and connected to an EASY-nLC 1000 instrument combined with an autosampler (Proxeon, Odense, Denmark). The HPLC was coupled to a QExactive plus mass spectrometer equipped with a nanoelectrospray ion source (Thermo Scientific, Rockford, USA). Peptides were loaded onto the column with 100% buffer A (99.9% H<sub>2</sub>O, 0.1% formic acid) and eluted at a constant flow rate of 300 nL min<sup>-1</sup> for 40 minutes with a linear gradient from 7-27% buffer B (99.9% acetonitrile, 0.1% formic acid), followed by 4 minutes from 27-35% buffer B and a washing step with 98% buffer B. Mass spectra were acquired in a data-dependent manner (Top12). In a standard method for medium to low-abundant samples high-resolution MS1 spectra were acquired @70,000 resolution (automatic gain control target value 3\*10<sup>6</sup>) to monitor peptide ions in the mass range of 375–1,500 m z<sup>-1</sup>, followed by HCD MS/MS scans @17,000 resolution (automatic gain control target value 1\*10<sup>6</sup>). To avoid multiple scans of dominant ions, the precursor ion masses of scanned ions are dynamically excluded from MS/MS analysis for 30 seconds. Single charged ions

and ions with unassigned charge states or charge states above 6 were excluded from MS/MS fragmentation. For data analysis, SEQUEST software v27.0<sup>29</sup> was used to search fragment ion spectra for a match to fully tryptic peptides without missed cleavage sites from a protein database, which was composed of the *Sus scrofa* proteome (SwissProt, organism ID 9823, 25.10.2015), various common contaminants and sequence-reversed decoy proteins. The precursor ion mass tolerance was set to 20 ppm. Carbamidomethylation was set as a fixed modification on all cysteines. The PeptideProphet and the ProteinProphet tools of the Trans-Proteomic Pipeline (TPP v4.6.2) were used for the probability scoring of peptides spectrum matches<sup>30</sup> and inferring protein identifications were filtered to reach an estimated false-discovery rate of  $\leq 1\%$ .

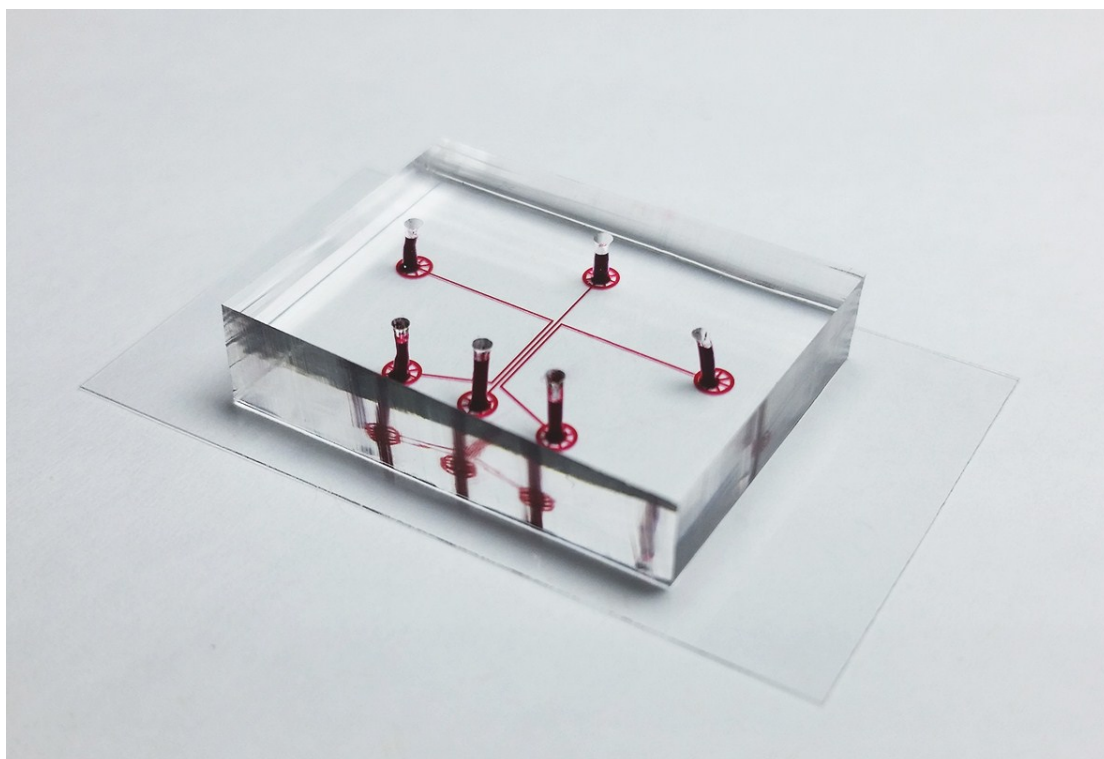


**Fig. S1 The assembled microfluidic chip.** The independent fluidic channels as well as the respective inlets and outlets are clearly visible. For clarity, the chip is shown without mounted reservoirs and channels are filled with red dye. The cover slip (24 x 40 mm) used as basis to the PDMS-microfluidic layer serves as size reference.

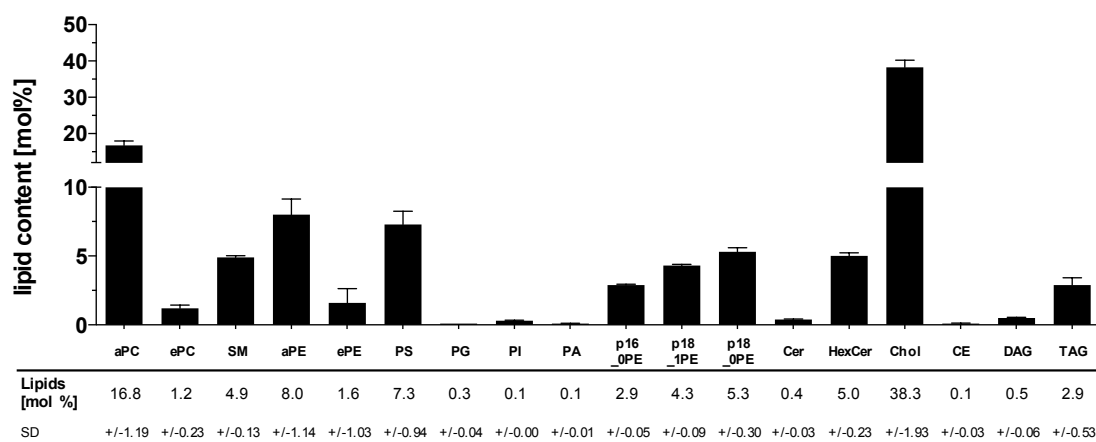


**Fig. S2 Detailed quantitative analysis of lipid constituents in NMN.** Relative amounts of the indicated lipids are depicted in mol%. Abbreviations for lipids are aPC (acylated phosphatidylcholine), ePC (1-ether phosphatidylcholine and di-acyl species containing one odd numbered fatty acid), SM (sphingomyelin), aPE (acylated phosphatidylethanolamine), ePE (1-ether phosphatidylethanolamine di-acyl species containing one odd numbered fatty acid), PS (phosphatidylserine), PG (phosphatidylglycerol), PI (phosphatidylinositol), PA (phosphatidic acid), pl-PE (phosphatidylethanolamine plasmalogen), Cer (ceramides), HexCer (hexosylceramides), Chol (cholesterol), CE (cholesterol fatty acid esters), DAG (diacylglycerols) and TAG (triacylglycerols), respectively (n = 3, mean  $\pm$  SD).

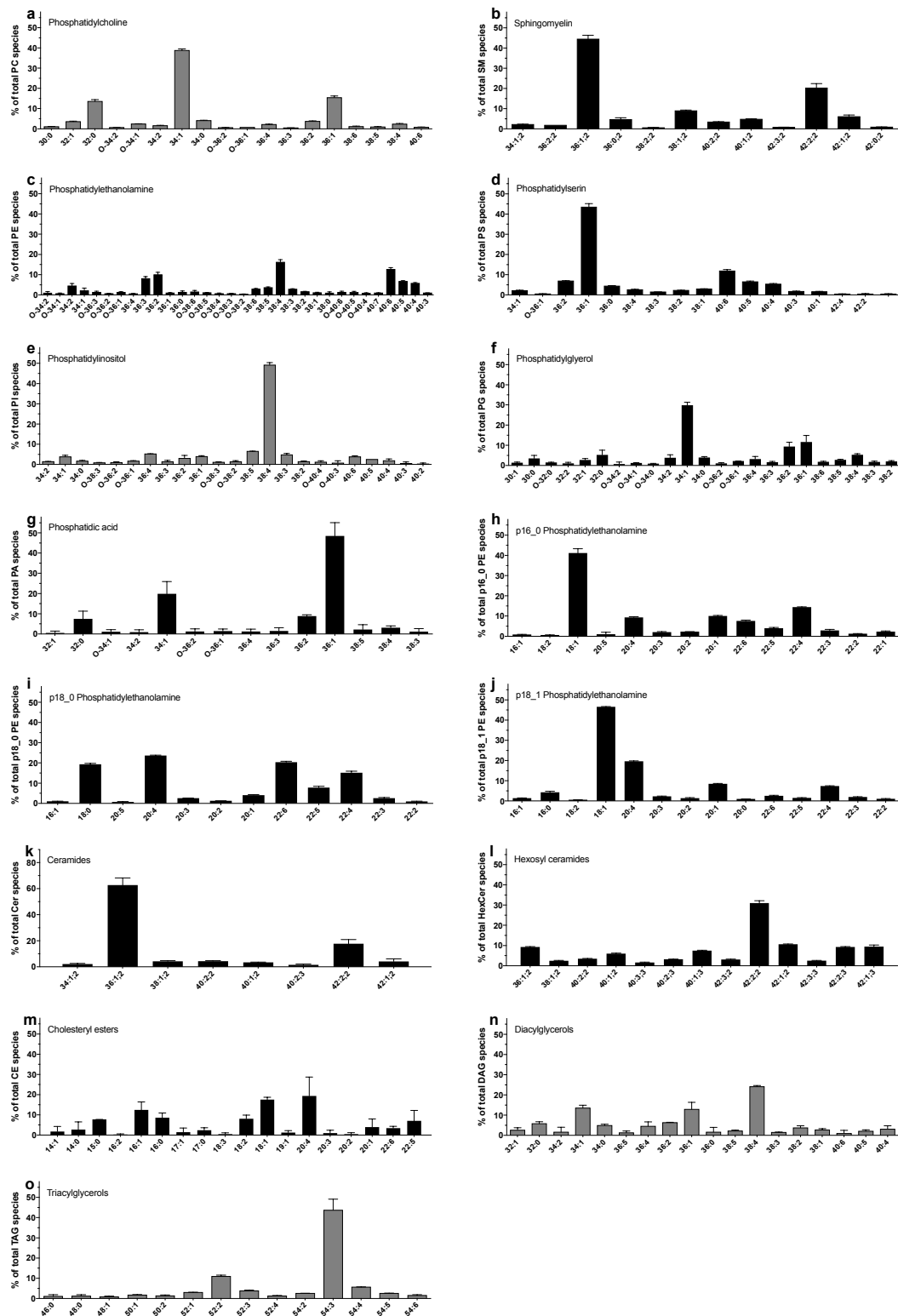


**Fig. S3 Analysis of lipid species distributions in NMN.** Relative amounts of lipid species are depicted in mol% with respective acyl chain lengths and number of double bonds. a) Phosphatidylcholine, b) Sphingomyelin, c) Phosphatidylethanolamine, d) Phosphatidylserine, e) Phosphatidylglycerol, f) Phosphatidylinositol, g) Phosphatidic acid, h) Phosphatidylethanolamine Plasmalogen p16\_0, i) Phosphatidylethanolamine Plasmalogen p18\_0, j) Phosphatidylethanolamine Plasmalogen p18\_1, k) Ceramides, l) Hexosyl ceramides, m) Cholesteryl esters, n) Diacylglycerols and o) Triacylglycerols. Grey bars represent data from neutral lipid extractions, black bars represents data from acidic lipid extraction (n = 3, mean  $\pm$  SD).

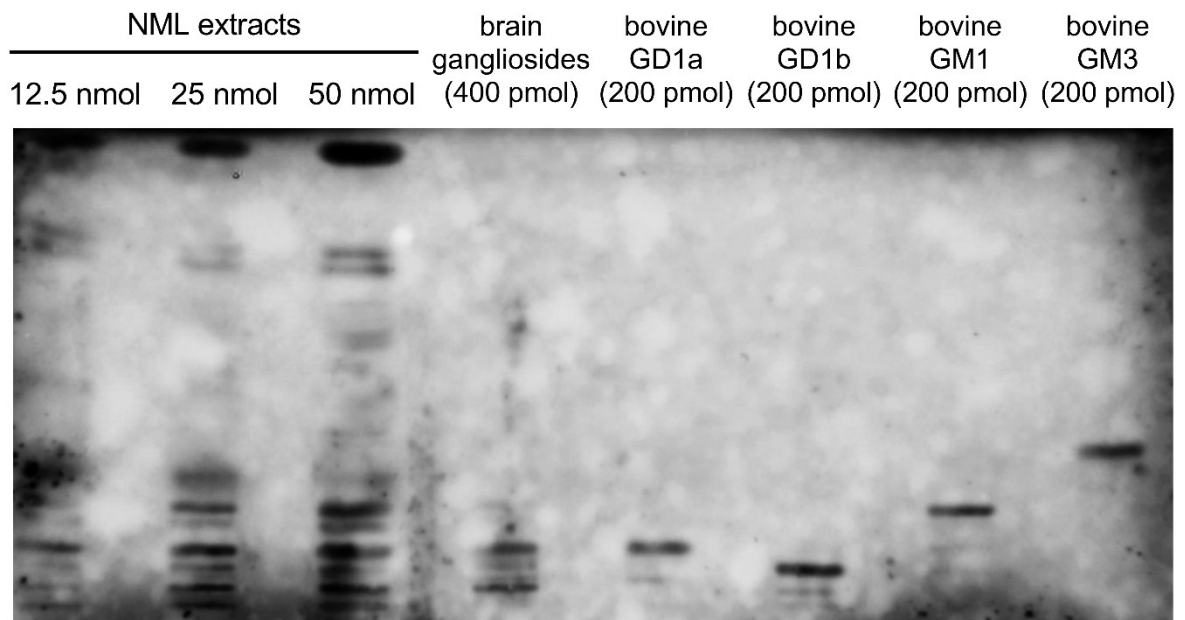


**Fig. S4. TLC-Analysis of ganglioside classes in NMN.** Ganglioside from NMN extracts (indicated amounts), respectively, were identified via thin layer chromatography and HCL-resorcinol staining and compared to a standard mixture of brain gangliosides and purified standards of individual ganglioside classes, respectively



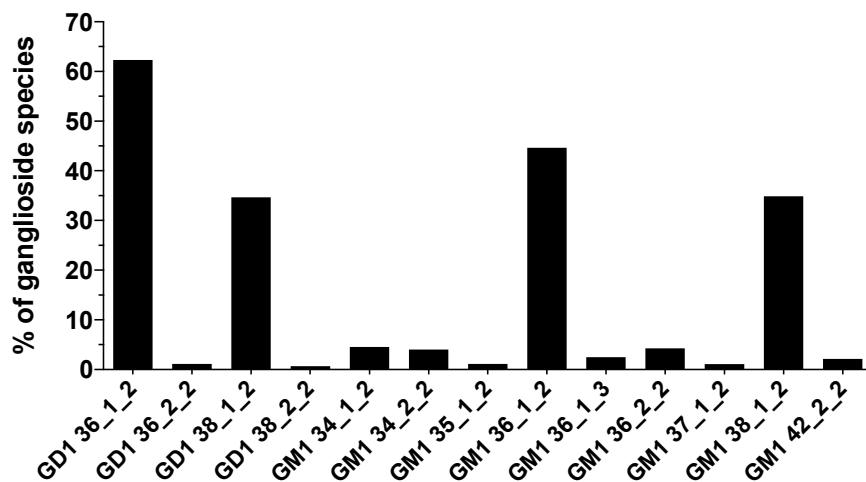


**Fig S5 MS-Analysis of Ganglioside species distribution in NMN.** Relative amounts of species of ganglioside classes a) GM1 and b) GD1 are depicted % of total species with respective acyl chain lengths, number of double bonds and number of hydroxylations given.

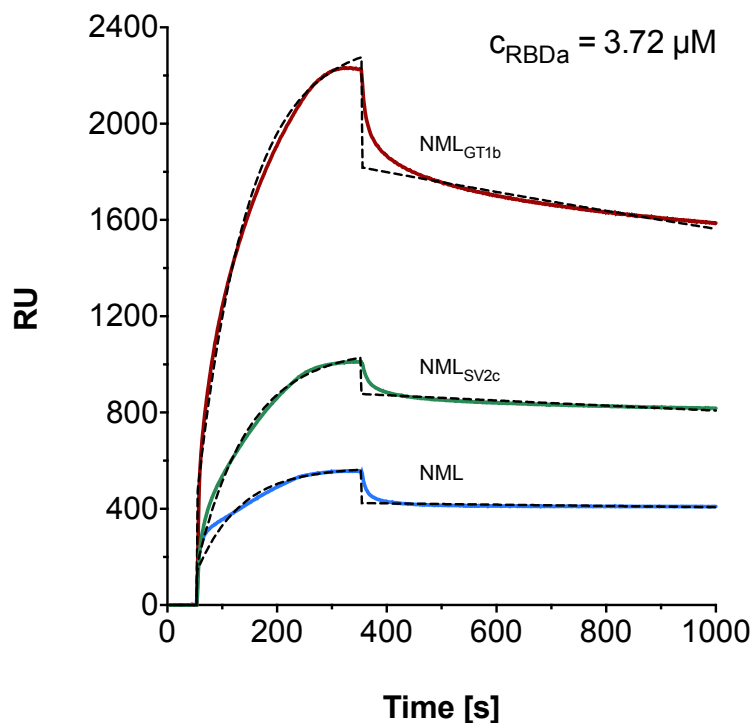


**Fig. S6 SPR binding kinetics of RBDA to NMN alone or supplemented with different receptors.** Sensograms for injections of RBDA, exemplarily shown for a concentration of  $3.72 \mu M$ , over a freshly prepared surface with either NMN (blue line), NMNSV2c (NMN supplemented with  $37 \text{ nM}$  human full length SV2c; Abnova, Taipei, Taiwan; green line), NMNGT1b (NMN supplemented with  $100 \mu M$  GT1b; Matreya, Pleasant Gap, USA; red line), respectively. Dashed lines represent kinetic curves fitted to a 1:1 kinetic-binding model. POPC-liposomes, containing no receptors, were used as reference channel.

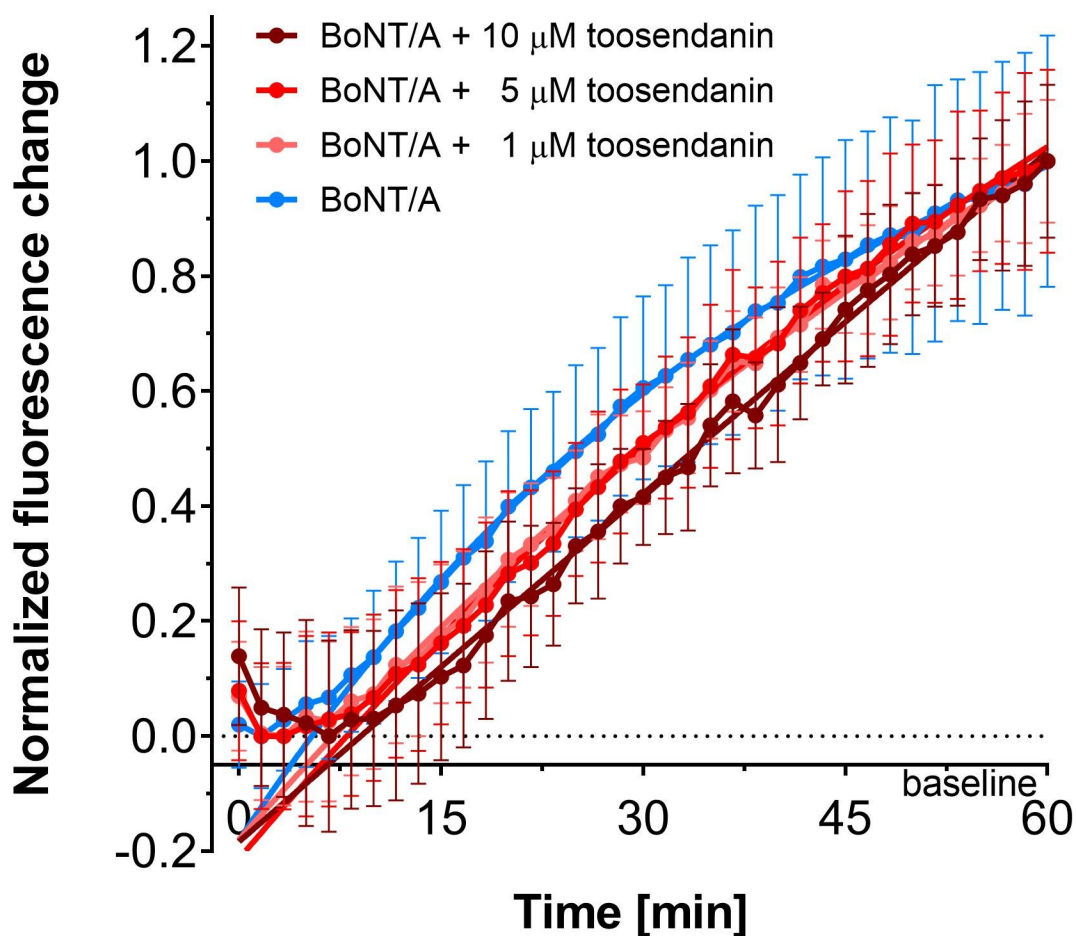


**Fig. S7. SNAPtide-cleavage by BoNT/A in presence of toosendanin.** Cleavage of 5  $\mu$ M SNAPtide in the presence of 100 ng BoNT/A and different concentrations of toosendanin was tested in reaction buffer in a total volume of 100  $\mu$ L at 37°C over 60 minutes and measured using a fluorescent plate reader. Background signal for buffer alone was subtracted, indicated by baseline (n = 2, mean  $\pm$  SD). Solid lines represent mathematical fits according to the Method section that was used to calculate half-lives.

**Tab. S1 Binding kinetic data at different concentrations of RBD<sub>A</sub> to NMN alone or supplemented with different receptors.**

<b>Concentration RBD<sub>A</sub> [<math>\mu</math>M]</b>	<b>NMN</b>		<b>NMN + SV2c</b>		<b>NMN + GT1b</b>	
	Average K <sub>D</sub>	SD	Average K <sub>D</sub>	SD	Average K <sub>D</sub>	SD
7.43 $\mu$ M	8.2E-08	3.0E-08	9.8E-08	8.2E-08	3.5E-07	3.0E-07
3.72 $\mu$ M	2.9E-07	1.5E-07	2.5E-07	3.7E-08	3.4E-07	2.1E-08
0.74 $\mu$ M	2.0E-08	4.0E-09	2.8E-08	1.3E-09	8.9E-07	2.2E-08
0.37 $\mu$ M	1.4E-08	1.3E-08	9.3E-11	5.3E-11	1.6E-08	8.1E-09

**Tab. S2 Half-times of intra-liposomal substrate conversion obtained for the indicated amounts of BoNT/A Holotoxin.**

<b>Concentration BoNT/A [pg]</b>	<b>Average half time [min]</b>	<b>SD</b>
<b>10000</b>	97.2	36.2
<b>1000</b>	113.3	29.5
<b>100</b>	149.3	29.6
<b>10</b>	215.9	30.5
<b>1</b>	233.2	22.8
<b>0</b>	275.7	47.9